



Influence of (E)-1-(2,4-dinitrophenyl)-2-[1-(2-nitrophenyl) ethylidene] hydrazine (DNPH) on the Hydrogen Evolution and Corrosion Inhibition of 18% Ni M 250 Grade weld aged Maraging steel in 0.5 M Sulfuric acid Medium at Different Temperatures

B. S. Sanatkumar^{1*} and A. Nityananda Shetty²

1. Department of Chemistry, National Institute of Technology Karnataka, Surathkal, Srinivasnagar-575 025, Karnataka, **INDIA**

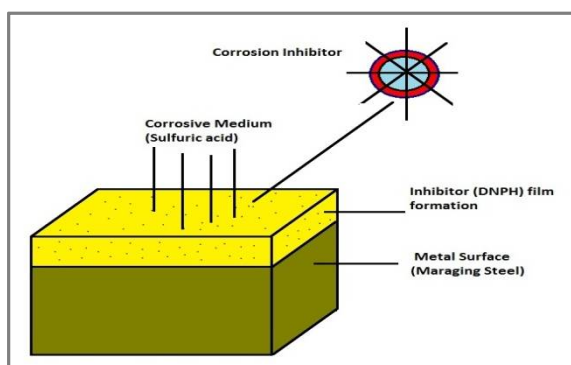
2. Department of Basic Science and Humanities, Agnel Institute of Technology and Design, Assagao, Bardez, Goa-403 507, **INDIA**
Email: sanatkumarbs@gmail.com

Accepted on 3rd February, 2019

ABSTRACT

The influence of (E)-1-(2,4-dinitrophenyl)-2-[1-(2-nitrophenyl) ethylidene] hydrazine (DNPH) on the corrosion of weld aged maraging steel in 0.5 M sulfuric acid medium was investigated by Tafel polarization curve and Electrochemical impedance spectroscopy (EIS) at different temperatures by varying the inhibitor concentrations. The results showed that the presence of DNPH hinders the rate of corrosion without altering the mechanism of anodic and cathodic reactions. The impedance parameters, such as charge transfer resistance (R_{ct}), double layer capacitance (C_{dl}), film capacitance (C_f) and film resistance (R_f) were extracted from Nyquist plot, they ensure the formation of protective film on the metal surface. DNPH act as a mixed type inhibitor without altering the mechanism of the hydrogen evolution reaction or metal dissolution. Scanning electron microscopy (SEM) and Energy dispersive X-ray spectroscopy (EDS) also confirms the formation of an adsorbed protective film on the metal surface.

Graphical Abstract



Schematic representation of the inhibition process.

Keywords: Maraging steel, DNPH, EIS, SEM, EDS.

INTRODUCTION

Maraging steel has gained more attention due to high strength and excellent fracture toughness [1]. The alloy is a low carbon steel that typically contain about 18 wt % Nickel, significant amount of Molybdenum, Cobalt and Titanium. The composition of the alloy can be altered based on the requirement and applications. Strength of the maraging steel can be increased by aging at 400-500°C, where intermetallics undergo precipitation [2]. Due to the low carbon content maraging steels possesses higher modulus of elasticity, lower thermal expansion coefficient, moderate toughness, good weld ability and machinability [3]. Many research reports revealed that maraging steels are widely used in the military, aircraft, aerospace tooling applications also in the preparation of nuclear and gas turbines [4-5]. Due to variety of applications and interaction with the corrosive environment, the corrosion of maraging steel is inevitable. According to Krick *et al.* maraging steel suffers from uniform corrosion when it is exposed to open atmosphere [6-7]. Bellanger *et al.* have studied the corrosion behavior of maraging steel in radioactive water and reported that reaction intermediates are responsible for passivation [8]. The influence of carbonate ions in slightly basic medium on the corrosion of maraging steel was studied by Bellanger [9]. Poornima *et al.* have studied the corrosion behavior of 18 Ni 250 grade maraging steel in sulfuric acid medium and reported that corrosion rate of the aged sample is more than annealed sample [7]. Similar observations also have been reported for the corrosion of 18 Ni 250 grade maraging steel in phosphoric acid medium [10]. The inhibitive action of 3,4 – dimethoxybenzaldehyde thiosemicarbazone on corrosion of aged maraging steel was studied by Poornima *et al* [11]. We have earlier reported the use of 2-(4-Chlorophenyl)-2-oxoethyl benzoate as an effective inhibitor for weld aged maraging steel in 1.0 M sulfuric acid medium [12]. Employing organic corrosion inhibitors on the metal surface is one of the most cost-effective and simple method to decrease the corrosion. The most well-known corrosion inhibitors are the compounds containing oxygen, nitrogen, sulphur, and phosphorus in their functional groups with aromatic and heterocyclic rings [13]. Majority of these organic compounds are adsorbed on the metal surface and form a barrier between metal surface and corrosion environment, hence mitigate the rate of corrosion [14-15]. The present research paper describes the corrosion inhibition behavior of (E)-1-(2,4-dinitrophenyl)-2-[1-(2-nitrophenyl) ethylidene] hydrazine (DNPH) on the corrosion of maraging steel in 0.5 M sulfuric acid medium at different temperatures by using Tafel polarization method, Electrochemical impedance spectroscopy, Scanning electron microscopy (SEM) and Energy Dispersive X- ray spectroscopy (EDS). The mode of adsorption and the corrosion inhibition mechanism are also discussed.

MATERIALS AND METHODS

Material: Tests were performed on 18% Ni M250 grade maraging steel under weld aged condition. The composition of the material is given in table 1. The test coupons were sealed with epoxy resin and leaving a constant surface area of 0.64 cm². These coupons were polished mechanically using different grades of abrasive papers and polishing wheel to obtain glossy surface. Finally washed with distilled water and degreased with acetone before being immersed in the corrosive medium. Experiments were carried out at different temperatures in the open atmosphere, under unstirred conditions.

Table 1. Composition of 18 % Ni M250 grade maraging steel (weight %)

Element	Composition	Element	Composition
C	0.015%	Ti	0.3-0.6%
Ni	17-19%	Al	0.005-0.15%
Mo	4.6-5.2%	Mn	0.1%
Co	7-8.5%	P	0.01%
Si	0.1%	S	0.01%
O	30 ppm	N	30 ppm
H	2.0 ppm	Fe	Balance

Medium: Standard solution of 0.5 M sulfuric acid was prepared by mixing analytical reagent grade sulfuric acid (Merck) and double distilled water. Inhibitive behaviour of DNPH on the corrosion of weld aged maraging steel in 0.5 M sulfuric acid was studied by adding different concentrations of the inhibitor into the solution. The tests were carried out at temperatures 30°C, 35°C, 40°C, 45°C and 50°C (± 0.5 °C), in a calibrated thermostat. The concentration range of DNPH prepared and used in this study was 0.3 mM -1.5 mM.

Synthesis of (E)-1-(2,4-dinitrophenyl)-2-[1-(2-nitrophenyl) ethylidene] hydrazine (DNPH): The inhibitor DNPH was synthesized as reported in the literature. A mixture of 2,4-dinitrophenylhydrazine (0.40 g, 2 mmol), ethanol (10.00 mL), H₂SO₄ (98%, 0.50 mL) and 2 Nitroacetophenone (0.27 mL, 2 m mol) was stirred and refluxed for 1 h. On cooling, yellow block-shaped single crystals of (E)-1-(2,4-DINITROPHENYL)-2-[1-(2-NITROPHENYL) ETHYLIDENE] was obtained [16]. The product was characterized by elemental analyses, melting point (170-171°C) and infrared spectra. The synthesis scheme is shown in figure 1.

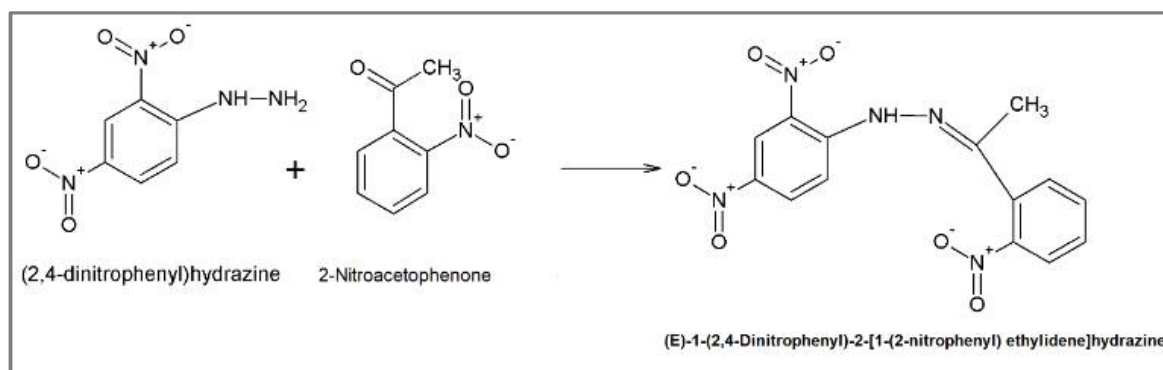


Figure 1. Synthesis scheme of (E)-1-(2,4-dinitrophenyl)-2-[1-(2-nitrophenyl) ethylidene] hydrazine (DNPH)

Electrochemical Measurements: Electrochemical measurements were performed by using Gill AC-ACM instrument. The experimental setup was arranged in such way that saturated calomel electrode (SCE) used as a reference electrode, platinum as counter-electrode and maraging steel as a working electrode. Tafel polarization experiments were carried out immediately after the EIS studies on the same electrode without any further surface treatment.

Tafel Polarization Studies: Nicely polished maraging steel specimen was exposed to the corrosion medium of 0.5 M sulfuric acid in the presence and absence of the inhibitor at different temperatures (30 - 50°C) and allowed to attain a steady-state open circuit potential (OCP). The Tafel curves were recorded by polarizing the metal specimen to -250 mV cathodically and +250 mV anodically with respect to the OCP at a scan rate of 1 mV s⁻¹.

Electrochemical Impedance Spectroscopy Studies (EIS): The electrochemical impedance measurements were performed in the frequency range of 10 KHz to 0.01 Hz, using Gill AC-ACM instrument by applying a sinusoidal perturbation of 10 mV. The values of double layer capacitance (C_{dl}), charge transfer resistance (R_{ct}), film capacitance (C_f) and film resistance (R_f) were extracted from the Nyquist plot. In all the above measurements, at least three similar results were considered, and their average values are reported.

Scanning electron microscopic (SEM) and EDS analysis: The SEM images were captured by using JEOL JSM - 6380LA scanning electron microscope. EDS analysis were performed to identify the elemental composition on the metal surface in the presence and absence of inhibitor. The exposure time of the electrode in acid medium for the SEM analysis was 4h.

RESULTS AND DISCUSSION

Tafel polarization measurement: Tafel polarization curves of weld aged maraging steel in 0.5 M sulfuric acid solution without and with different concentrations of DNPH at 30°C were shown in figure 2. Similar plots were gathered at other temperatures also. Electrochemical parameters, such as corrosion current density (i_{corr}), corrosion potential (E_{corr}), inhibition efficiency η (%), cathodic and anodic Tafel slopes (b_c and b_a) calculated from Tafel plots are listed in table 2.

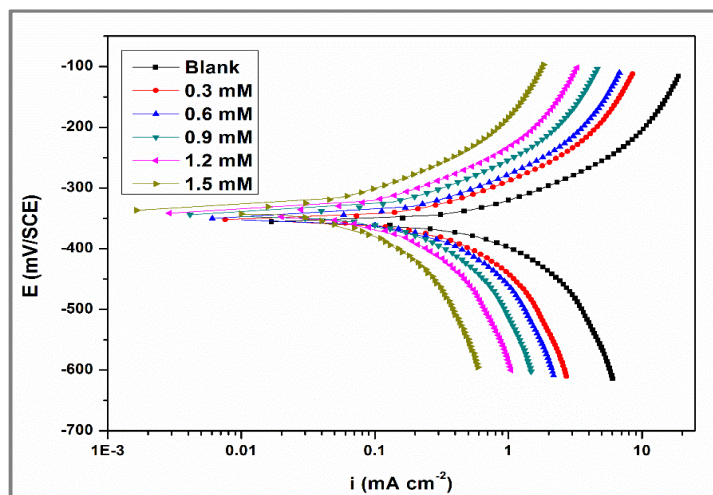


Figure 2. Tafel polarization curves for the corrosion of weld aged maraging steel in 0.5 M sulphuric acid containing different concentrations of DNPH at 30°C.

The inhibition efficiency was calculated from following equation [17]:

$$\eta(\%) = \frac{i_{corr} - i_{corr(inh)}}{i_{corr}} \times 100 \quad (1)$$

Where i_{corr} and $i_{corr(inh)}$ are the corrosion current densities obtained in the absence and presence of inhibitors, respectively. It is very clear from the data shown in Table 2, presence of inhibitor brings down the corrosion rate significantly. Polarization curves are shifted towards lower current density region indicating decrease in the corrosion rate (v_{corr}). Inhibition efficiency increases with the increase in DNPH concentration. The higher inhibition efficiency can be attributed to the adsorption of inhibitor molecule through polar groups as well as through π - electrons of the double bond. There is no appreciable change in the values of cathodic and anodic Tafel slope (b_c & b_a) with the increase in the concentration of the inhibitor. This suggests that metal dissolution and hydrogen evolution reactions were decreased after the addition of DNPH to the corrosive solution [18-19]. The optimum quantity of the inhibitor is listed in table 2. There is no significant change in the E_{corr} values, both the cathodic and anodic polarization patterns were slightly altered together, this shows inhibitive action of DNPH on the metal surface. Suppose the change in corrosion potential is higher than ± 85 mV with respect to the corrosion potential of the acid solution, the inhibitor can be considered as either cathodic or anodic type.

However, the maximum change in this analysis is ± 20 mV; and therefore, DNPH can be considered as a mixed type inhibitor [20-21]. The inhibitive property of DNPH can be considered due to the adsorption and formation of film on the metal surface. The inhibitor layer formed on the metal surface diminishes the feasibility of both the cathodic and anodic reactions.

Table 2. Results of Tafel polarization studies for the corrosion of weld aged maraging steel in 0.5 M sulphuric acid containing different concentrations of DNPH

Temperature (°C)	Conc. of inhibitor (mM)	E_{corr} (mV/SCE)	b_a (mV dec ⁻¹)	$-b_c$ (mV dec ⁻¹)	i_{corr} (mA cm ⁻²)	v_{corr} (mm y ⁻¹)	η (%)
30	Blank	-356	235	268	1.80	20.71	--
	0.3	-352	232	263	0.63	7.27	64.9
	0.6	-350	226	257	0.50	5.70	72.5
	0.9	-344	222	253	0.39	4.49	78.3
	1.2	-342	219	248	0.26	2.98	85.6
	1.5	-339	217	247	0.14	1.57	92.4
35	Blank	-353	257	276	2.41	27.73	--
	0.3	-348	252	273	0.89	10.27	63.0
	0.6	-345	246	267	0.71	8.21	70.4
	0.9	-340	242	264	0.57	6.59	76.3
	1.2	-337	237	261	0.39	4.54	83.6
	1.5	-337	236	259	0.23	2.64	90.5
40	Blank	-350	279	288	3.83	44.07	--
	0.3	-345	277	283	1.52	17.46	60.4
	0.6	-342	270	277	1.23	14.16	67.9
	0.9	-337	267	273	1.00	11.55	73.8
	1.2	-336	264	268	0.72	8.27	81.2
	1.5	-332	262	267	0.45	5.22	88.2
45	Blank	-348	296	297	4.01	46.14	--
	0.3	-341	291	295	1.68	19.33	58.1
	0.6	-339	285	289	1.38	15.83	65.7
	0.9	-333	281	286	1.14	13.08	71.7
	1.2	-333	276	283	0.83	9.61	79.2
	1.5	-330	275	281	0.55	6.38	86.2
50	Blank	-346	315	306	4.30	49.47	--
	0.3	-341	313	301	1.95	22.48	54.6
	0.6	-340	307	295	1.63	18.70	62.2
	0.9	-335	304	291	1.37	15.71	68.2
	1.2	-334	301	286	1.04	11.95	75.8
	1.5	-333	299	285	0.73	8.46	82.9

Electrochemical impedance spectroscopy studies (EIS): Nyquist plots for the corrosion of maraging steel in 0.5 M sulfuric acid solution containing various concentrations of DNPH were shown in figure 3. The parameters, such as charge transfer resistance (R_{ct}), Double layer capacitance (C_{dl}), film capacitance (C_f) and film resistance (R_f) and inhibition efficiency values η (%) calculated are listed in Table 3. Even at higher temperature similar plots were obtained. From figure 3, it can be observed that the impedance spectra exhibit a single semicircle and the diameter of semicircle increases with increasing inhibitor concentration. This indicates that the corrosion of weld aged maraging steel is controlled by a charge transfer process and the addition of DNPH does not change the reaction mechanism of the corrosion of sample in sulfuric acid solution. The impedance spectra did not present perfect semicircles, the depressed semicircle was often attributed to the surface roughness, dislocations and distribution of the active sites or adsorption of inhibitors [11]. As R_{ct} is inversely proportioned to the corrosion current density, inhibitor efficiency, η (%) was calculated from the following relationship [22]:

$$\eta(\%) = \frac{R_{ct(inh)} - R_{ct}}{R_{ct(inh)}} \times 100 \quad (2)$$

Where $R_{ct(inh)}$ and R_{ct} are the charge transfer resistances obtained in inhibited and uninhibited solutions, respectively.

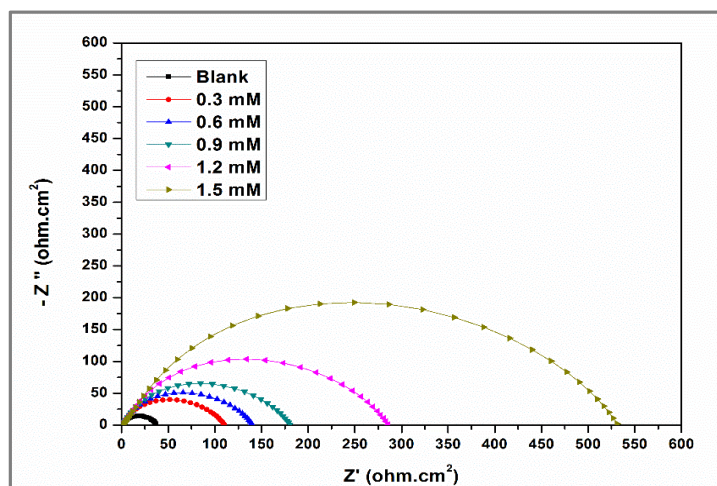


Figure 3. Nyquist plots for the corrosion of weld aged maraging steel in 0.5 M sulphuric acid containing different concentrations of DNPH at 30.

Table 3. EIS data for the corrosion of weld aged maraging steel in 0.5 M sulphuric acid containing different concentrations of DNPH.

Temperature (°C)	Conc. of inhibitor (mM)	R_{ct} (ohm. cm ²)	C_{dl} (mF cm ⁻²)	R_f (ohm. cm ²)	C_f (mF cm ⁻²)	η (%)
30	Blank	33.56	4.01	--	--	--
	0.3	100.39	1.70	8.10	0.51	66.6
	0.6	130.28	1.36	9.93	0.42	74.2
	0.9	168.64	1.10	12.29	0.34	80.1
	1.2	267.84	0.78	18.40	0.26	87.5
	1.5	592.93	0.47	38.40	0.17	94.3
35	Blank	26.64	6.59	--	--	--
	0.3	75.08	2.56	6.54	0.75	64.5
	0.6	95.14	2.07	7.77	0.62	72.0
	0.9	120.65	1.68	9.34	0.51	77.9
	1.2	182.09	1.19	13.12	0.37	85.4
	1.5	345.97	0.73	23.20	0.24	92.3
40	Blank	17.85	10.98	--	--	--
	0.3	47.21	4.27	4.82	1.23	62.2
	0.6	59.03	3.46	5.55	1.01	69.8
	0.9	73.58	2.82	6.45	0.83	75.7
	1.2	106.63	2.02	8.48	0.60	83.3
	1.5	183.26	1.27	13.19	0.39	90.3
45	Blank	17.84	12.56	--	--	--
	0.3	44.27	5.40	4.64	1.55	59.7
	0.6	54.62	4.42	5.28	1.28	67.3
	0.9	67.02	3.64	6.04	1.06	73.4
	1.2	93.80	2.67	7.69	0.79	81.0
	1.5	149.29	1.76	11.10	0.53	88.1
50	Blank	17.42	15.83	--	--	--
	0.3	39.47	7.48	4.35	2.14	55.9
	0.6	47.84	6.21	4.86	1.78	63.6
	0.9	57.47	5.21	5.45	1.50	69.7
	1.2	76.94	3.95	6.65	1.14	77.4
	1.5	112.46	2.77	8.84	0.81	84.5

Increase in the value of charge transfer resistance (R_{ct}) and decrease in C_{dl} double layer capacitance also conforms the formation of electrical double layer and adsorption of DNPH molecules on the metal surface. The data shown in table 3 reveal that the charge transfer resistance (R_{ct}) and film resistance (R_f), increases with the increase in the inhibitor concentration, suggesting an hindrance to the charge transfer reaction (i.e., effective metal dissolution) [19]. The increase in R_{ct} , R_f and decrease C_{dl} and C_f values is due to the gradual replacement of water molecules by the adsorption of the inhibitor molecules on the metal surface to form an adherent film on the metal surface and thereby reducing the metal dissolution in the solution [20].

The obtained Bode plot for DNPH is shown in figure 4. The high frequency (HF) limits correspond to R_s (Ω), while the lower frequency (LF) limits corresponds to ($R_{ct} + R_s$), which is allied with the dissolution processes at the interface. The low frequency contribution shows the kinetic response of the charge transfer reaction. Phase angle increases with increase in concentrations of DNPH in sulphuric acid medium. This might be due to decrease in dissolution of metal and decrease in capacitive behaviour on the metal surface.

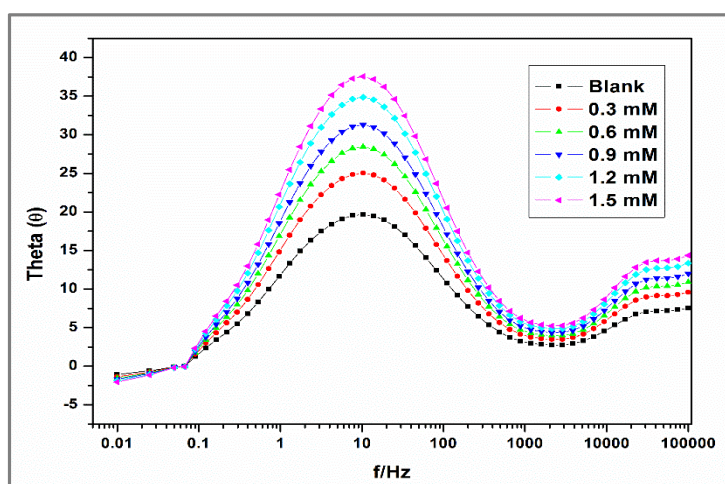


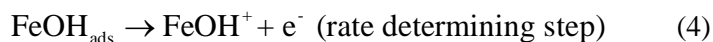
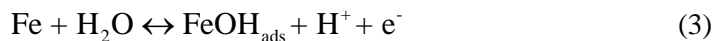
Figure 4. Bode plots for the corrosion of weld aged maraging steel in 0.5 M sulphuric acid containing different concentrations of DNPH at 30°C.

The presence of one phase maximum at intermediate frequencies indicates the presence of single time constant corresponding to the impedance of the formed adsorbed film. The difference between the HF and LF for the inhibited system in the Bode plot increases with increase in the concentration of DNPH [22]. At the highest inhibitor concentration of 1.5 mM, the inhibition efficiency was increased noticeably and reached 94.3%. Furthermore, the values of inhibition efficiency obtained Tafel polarization measurements and EIS measurements are identical to each other.

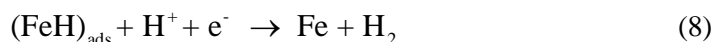
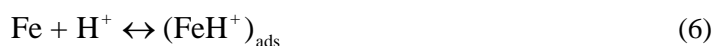
Effect of temperature: The results of Tafel polarization and electrochemical impedance spectroscopy given in tables 2 and 3 shows that inhibition efficiency of DNPH decreases with increase in temperature. In this study, with increase in solution temperature, corrosion potential (E_{corr}), anodic Tafel slope (b_a), and cathodic Tafel slope (b_c) values are not altered much. This shows that increase in temperature does not change the mechanism of corrosion reaction. However, I_{corr} and the corrosion rate of the metal increases with increase in temperature for both inhibited and uninhibited solutions. The inhibition efficiency decreases with increase in temperature which indicates desorption of inhibitor molecules. [23, 24]. This may be due to the higher dissolution rates of weld aged maraging steel at higher temperature and also a possible desorption of adsorbed inhibitor due to increased solution agitation resulting from higher rates of hydrogen gas evolution, which may also reduce the ability of the inhibitor to be adsorbed on the metal surface. The decrease in R_{ct} and inhibition efficiency with the increase in temperature indicates desorption of the inhibitor molecules from the metal surface

on increasing the temperature. This phenomenon also indicates the physisorption of the inhibitor molecules on the metal surface [25-27].

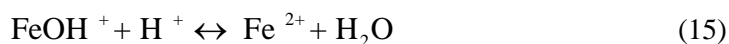
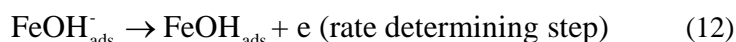
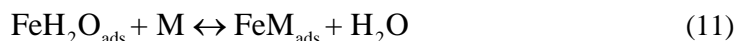
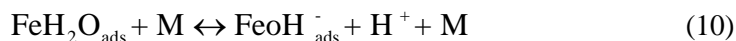
Mechanism of corrosion inhibition: The adsorption mechanism of an inhibitor depends on factors, such as the nature of the metal, the corrosive medium, the pH, and the concentration of the inhibitor as well as the functional groups present in its molecule, since different groups are adsorbed to different extents. According to Bockris *et al.* and Obot *et al.*, the metal dissolution and inhibition action was followed by the following mechanism [28]:



The cathodic hydrogen evolution follows the steps



The following mechanism involving two adsorbed intermediates to account for the retardation of Fe anodic dissolution in the presence of an inhibitor:



Where M represents the inhibitor species, according to the above exhaustive mechanism, displacement of some adsorbed water molecules on the metal surface by inhibitor species to yield the adsorbed intermediate FeM_{ads} reduces the amount of the species $\text{FeOH}_{\text{ads}}^-$ available for the rate determining steps and consequently retards Fe anodic dissolution [29-30].

SEM/EDS studies: The scanning electron microscope images were recorded to establish the interaction of acid solution with the metal surface. Figure 5(a) represents the SEM image of the

corroded weld aged maraging steel sample which shows the facets due to the attack of sulphuric acid on the metal surface with cracks and rough surfaces. Figure 5(b) shows the SEM image of the sample after immersion in 0.5 M sulphuric acid in the presence of DNPH. The alloy surface is smooth without any visible corrosion attack. The image clearly shows the adsorbed layer of inhibitor molecules on the alloy surface thus protecting the metal from corrosion [31-33].

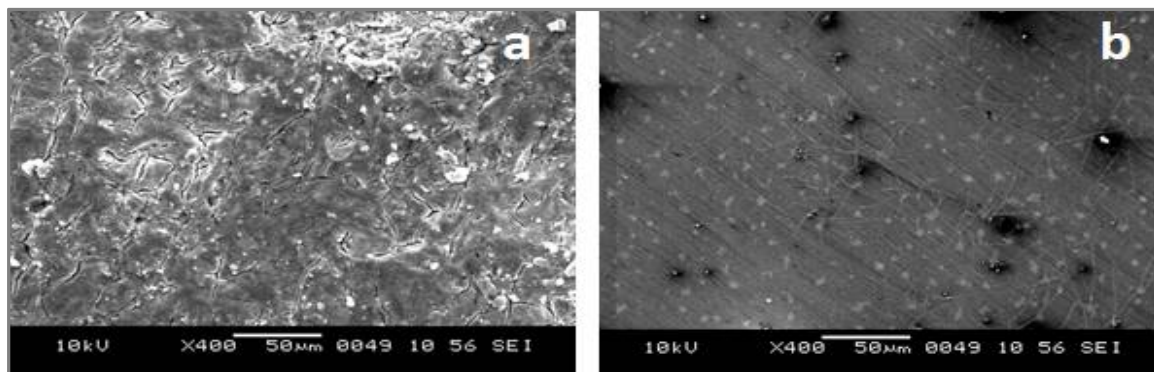


Figure 5. SEM images of the weld aged maraging steel after immersion in 0.5 M sulphuric acid
a) in the absence and b) in the presence of DNPH.

The corresponding EDS profile analyses for the selected areas on the SEM images 5(a) and 5(b) are shown in figure 6(a) and figure 6(b), respectively. The atomic percentage of the elements found in the EDS profile for corroded metal surface were 12.11 % Fe, 3.87 Ni, 4.92% Mo, 73.15% O, 1.72 % Co and 6.50% S and indicated that iron oxide is existing in this area. These elemental compositions prove that the corrosion of weld aged maraging steel through the formation of oxide layer. The atomic percentage of the elements found in the EDS profile for less uncorroded metal surface were 4.52 % Fe, 0.71% Ni, 1.77% Mo, 53.13 % O, 1.18% Cl, 31.42% C and 5.47% S and indicated that formation of inhibitor film in this area. The elemental composition mentioned above was mean value of different regions.

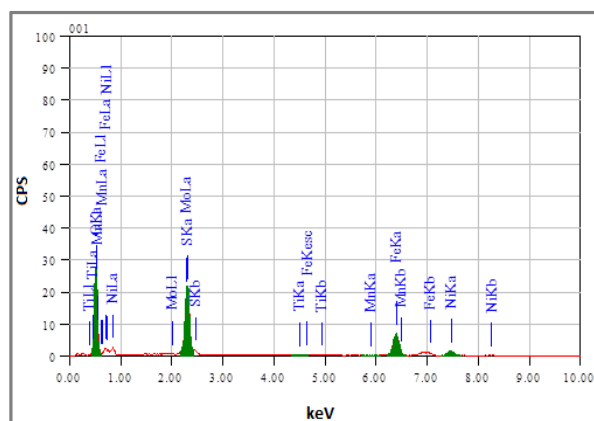


Figure 6(a). EDS spectra of the weld aged maraging steel after immersion in 0.5 M sulphuric in the absence of DNPH

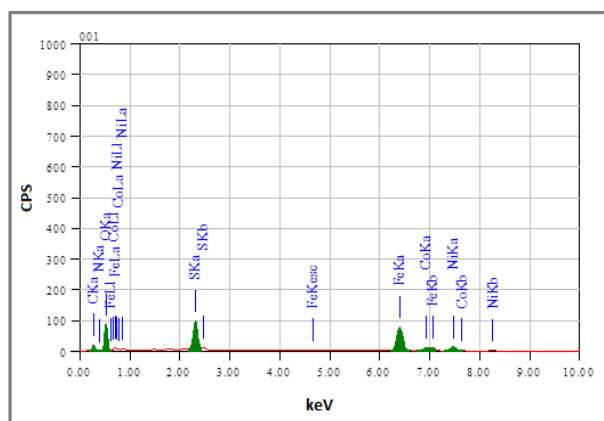


Figure 6(b). EDS spectra of the weld aged maraging steel after immersion in 0.5 M sulphuric in the presence of DNPH.

APPLICATION

Maraging steels are used in the fabrication of rocket and missile skins in aerospace industries. Due to the low carbon content, maraging steels have good machinability. Its strength and malleability allow it to be used in the preparation engine components like crankshafts and gears, bicycle frames, wheel bearings, ship hulls, medical components, nuclear and gas turbine applications.

CONCLUSION

The following conclusions may be drawn from the study:

1. The DNPH acts as a mixed type inhibitor, which affect both anodic dissolution of weld aged maraging steel and hydrogen evolution reactions.
2. The polarisation results reveal that corrosion current density (i_{corr}) value or hydrogen evolution rate increases with either increasing temperature or decreasing inhibitor concentration.
3. The EIS results showed that Charge transfer (R_{ct}) value increases with increasing inhibitor concentration indicating hindrance for cathodic reduction and metal dissolution, suggesting decrease in corrosion rate.
4. The results obtained from Tafel polarization and EIS studies are identical to each other.
5. The SEM/EDX inspection proves that the inhibition of corrosion is due to formation of an adsorbed passive film on the metal surface.

REFERENCES

- [1]. C. Menapace, I. Lonardelli, A. Molinari, Phase transformation in a nanostructured M300 maraging 22 steel obtained by SPS of mechanically alloyed powders, *J. Therm. Anal. Calorim*, **2010**, 101, 815
- [2]. K. Stiller, F. Danoix, A. Bostel, Investigation of precipitation in a new maraging stainless steel, *20 Appl. Surf. Sci.*, **1996**, 94, 326.
- [3]. W. Wang, W. Yan, Q. Duan, Y. Shan, Z. Zhang, K. Yang, Study on fatigue property of a new 2.8 26 GPa grade maraging steel, *Mater. Sci. Eng. A*, **2010**, 527, 3057- 3063.
- [4]. S. Hossein Nedjad, J. Teimouri, A.Tahmasebifar, H. Shirazib, M. Nili Ahmadabadi, A new concept 28 in further alloying of Fe-Ni-Mn maraging steels, *Scr. Mater*, **2009**, 60, 528–531.
- [5]. T. Poornima, J. Nayak, A.N. Shetty, Studies on corrosion of annealed and aged 18 ni 250 grade 30 maraging steel in sulphuric acid medium, *Port. Electrochim. Acta*, **2010**, 28(3), 173-188.
- [6]. W. W. Krick, R. A.Covert, T. P. May, Corrosion behavior of high strength steels in marine 32 environment, *Met Eng Quart.*, **1968**, 8, 31.
- [7]. B. S. Sanatkumar, J. Nayak, A. N. Shetty, Corrosion Behavior of 18% Ni M250 Grade Maraging Steel Under Weld-Aged Condition in Sulfuric Acid Medium, *Chem. Eng. Commun.* **2012**, 199, 1610–1625.
- [8]. G. Bellanger, J. J. Rameau, Effect of slightly acid pH with or without chloride in radioactive water 36 on the corrosion of maraging steel, *J. Nucl. Mater*, **1996**, 228, 24.
- [9]. G. Bellanger, Effect of carbonate in slightly alkaline medium on the corrosion of maraging steel, *J.Nucl. Mater*, **1994**, 217, 187.
- [10]. T. Poornima, J. Nayak, A. N. Shetty, Corrosion of aged and annealed 18 Ni 250 grade maraging 40 steel in phosphoric acid medium, *Int. J. Electrochem. Sci*, **2010**, 5, 56 –71.
- [11]. T. Poornima, J. Nayak, A. N. Shetty, 3, 4 - Dimethoxy benzaldehyde thiosemicarbazone as 42 corrosion inhibitor for aged 18Ni 250 grade maraging steel in 0.5 M sulfuric acid, *J. Appl. Electrochem.*, **2011**, 41, 223 - 233.
- [12]. B. S. Sanatkumar, J. Nayak, A. N. Shetty, The corrosion inhibition of maraging steel under weld 1 aged condition by 1(2E)-1-(4-aminophenyl)-3-(2-thienyl)prop-2-en- 1-one in 1.5 M hydrochloric 2 acid medium, *J. Coat. Technol. Res*, **2012**, 9, 483-493.
- [13]. N. N. Greenwood, A. Earnshaw, Chemistry of the elements. 2nd ed. Great Britain, Pergamon, **1998**.
- [14]. F. Bentiss, M. Lebrini, M. Lagrenee, Thermodynamic Characterization of Metal Dissolution and Inhibitor Process in Mild Steel/2,5-bis(n-Thienyl)-1,3,4-thiadiazoles/Hydrochloric Acid System, *Corros. Sci.*, **2005**, 47, 2915-2931.
- [15]. S. S. Abd El-Rehim, M. A. M. Ibrahim, K. F. Khaled, 4-Aminoantipyrine as an Inhibitor of Mild Steel Corrosion in HCl Solution, *J. Appl. Electrochem.*, **1999**, 29, 593-599.

- [16]. Boonlerd Nilwanna, Suchada Chantrapromma, Patcharaporn Jansrisewangwonga and Hoong-Kun Funb, (E)-1-(2,4-Di-nitro-phen-yl)-2-[1-(2 nitro-phen-yl)ethyl-iden]hydrazine, *Acta Crystallographica Section E*, **2011**, 67, 3084-3085.
- [17]. R. A. Prabhu, A. V. Shanbhag, T. V. Venkatesha, Influence of tramadol [2-[(dimethylamino) methyl] 1-(3- methoxyphenyl) cyclohexanol hydrate] on corrosion inhibition of mild steel in acidic media, *J. Appl. Electrochem.*, **2007**, 37, 491-497.
- [18]. G. Avci, Corrosion inhibition of indole-3-acetic acid on mild steel in 0.5 M HCl, *Colloids Surf. A*, **2008**, 317, 730-736.
- [19]. B. S. Sanatkumar , Jagannath Nayak , A. Nityananda Shetty, Influence of 2-(4-chlorophenyl)-2-oxoethyl benzoate on the hydrogen evolution and corrosion inhibition of 18 Ni 250 grade weld aged maraging steel in 1.0 M sulfuric acid medium, *Int. J. Hydrog. Energy* , **2012**, 37, 9431-9442.
- [20]. F. Nada Atta, A. M. Fekry, M. Hamdi Hassaneen. Corrosion inhibition, hydrogen evolution and antibacterial properties of newly synthesized organic inhibitors on 316L stainless steel alloy in acid medium, *Int. J. Hydrog. Energy*, **2011**, 1-10.
- [21]. Wei-hua Li, Qiao He, Sheng-tao Zhang, Chang-ling Pei, Bao-rong Hou. Some new triazole derivatives as inhibitors for mild steel corrosion in acidic medium, *J. Appl. Electrochem.*, **2008**, 38, 289–295.
- [22]. Xiumei Wang, Huaiyu Yang, Fuhui Wang, A cationic gemini-surfactant as effective inhibitor for mild steel in HCl solutions, *Corros. Sci.*, **2010**, 52, 1268-1276.
- [23]. A. S. Fouda, F. E. Heikal, M. S. Radwan, Role of some thiadiazole derivatives as inhibitors for the corrosion of C-steel in 1 M H₂SO₄, *J. Appl. Electrochem.*, **2009**, 39, 391-402.
- [24]. M. P. Geetha, J. Nayak, A. N. Shetty. Corrosion inhibition of 6061Al-15vol.pct.SiC(p) composite and its base alloy in a mixture of sulphuric acid and hydrochloric acid by 4-(N,N-dimethylamino) benzaldehyde thiosemicarbazone, *Mater. Chem. Phys.*, **2011**, 125, 628-640.
- [25]. T. Sanaa Arab, Inhibition action of thiosemicarbazone and some of its r-substituted compounds on the corrosion of iron-base metallic glass alloy in 0.5 M H₂SO₄ at 30°C, *Mater. Res. Bull.*, **2008**, 43, 510-521.
- [26]. Wei-hua Li, Qiao He, Sheng-tao Zhang, Chang-ling Pei, Bao-rong Hou. Some new triazole derivatives as inhibitors for mild steel corrosion in acidic medium. *J. Appl. Electrochem.*, **2008**, 38, 289-295.
- [27]. B. S. Sanatkumar , Jagannath Nayak , A. Nityananda Shetty, Corrosion Inhibition, Hydrogen Evolution and Adsorption Properties of 2-(4-8 Bromophenyl)-2-Oxoethyl 4-Chlorobenzoate on the Corrosion of the 18% Ni M2 50 Grade Maraging Steel under Weld Aged Condition in 2.0 M HCl 1.0 Solution, *J. Applicable Chem.*, **2017**, 6(2), 241-264.
- [28]. I. B. Obot, N. O. Obi-Egbedi, A. O. Eseola, Anticorrosion potential of 2-Mesityl-1H-imidazo[4,5-f][1,10]- phenanthroline on mild steel in sulfuric acid solution, Experimental and theoretical study, *Ind. Eng. Chem. Re.s*, **2011**, 50, 2098-2110.
- [29]. A. S. Fouda, G. Y.Elawady, W. T. Elbehairy, Adsorption and Protection of Low C-Steel Corrosion in 1M Hydrochloric acid Medium using Hyosecyamus Muticus Plant Extract, *J. Applicable Chem.*, 2017, 6(1), 69-83.
- [30]. S. K. Rajappa, T. V. Venkatesh, Corrosion Protection Studies of Modified Mild Steel Surface in Hydrochloric Acid Medium, *J. Applicable Chem.*, **2015**, 4(1), 212-220.
- [31]. Sanaulla Pathapalya Fakrudeen, V. Bheema Raju, Inhibitive effect of N,N'-bis(Salicylidene)-1,2-Diaminoethane and N,N'-bis(3- Methoxy Salicylidene)-1,2-Diaminoethane on the corrosion of AA6061 alloy in Hydrochloric acid, *J. Applicable Chem.*, 2013, 2(4), 940-957.
- [32]. Preethi Kumari P, Prakash Shetty, Suma A Rao, Corrosion Inhibition of Mild Steel in HCl Medium by 2-(3, 4, 5-Trimethoxybenzylidene) Hydrazinecarbothioamide, *J. Applicable Chem.*, 2014, 3(1), 385-396.
- [33]. A. S. Fouda, S. Abd El-Maksoud, S.A. Gomaa, A.Elsalakawy, Thiophene Derivatives as Corrosion Inhibitors for CS in 0.5 M H₂SO₄ Solutions, *J. Applicable Chem.*, 2017, 6(1), 160-175.